Nuclear Engineering and Design 323 (2017) 39–45

Contents lists available at ScienceDirect

Nuclear Engineering and Design

journal homepage: www.elsevier.com/locate/nucengdes

Experimental study on the content and distribution of key nuclides in an irradiated graphite sphere of HTR-10

Hong Li, Xuegang Liu, Feng Xie*, Fuming Jia

Institute of Nuclear and New Energy Technology, Collaborative Innovation Center of Advanced Nuclear Energy Technology, Key Laboratory of Advanced Reactor Engineering and Safety of Ministry of Education, Tsinghua University, Beijing 100084, China

ARTICLE INFO

Keywords:
HTR-10
An irradiated graphite sphere
Radial distribution
H-3
C-14

ABSTRACT

An irradiated graphite sphere of the 10 MW high temperature gas-cooled reactor (HTR-10) has been studied experimentally with a mechanical disintegration way and a suite of radiochemical analysis methods, including the total α/β counting measurement and the absolute activity measurement with a liquid scintillation counter and a high-purity germanium detector connected to a multichannel analyzer. The key nuclides in this irradiated graphite sphere were determined, which were H-3, C-14, Co-60, and Cs-137. The radial distributions of the specific activity for each nuclide were obtained experimentally and compared with theoretical calculations. The production mechanisms of H-3, C-14, Co-60, and Cs-137 in the irradiated graphite sphere of HTR-10 were discussed individually, and the generation sources for each nuclide were analyzed explicitly. Current results can supply important experimental data for source term analysis of HTR-10, and provide useful research reference for the decommissioning work and waste minimization of high temperature gas-cooled reactors (HTGRs).

1. Introduction

The Very High Temperature Gas Cooled Reactor System (VHTR), as a development of high temperature gas-cooled reactors (HTGRs), has been selected for a candidate of the Generation IV systems by the Generation IV International Forum (GIF) for the production of process heat, electricity, and hydrogen (NERAC and GIF, 2002). A high level of passive safety performance, high generating efficiency, and high temperature heat output promise a broad commercial utilization for HTGRs (Zhang and Yu, 2002). For the pebble bed high temperature gas cooled reactor, the performance of the fuel spheres in the core plays a crucial role with regard to nuclear safety. The nuclides produced in the core are the original source of radioactive substances into primary coolant and auxiliary systems in a nuclear power plant. Thus, the determination of the source term in the reactor core can supply important information to understand the behavior of fission and activation products and provide reliable foundation to evaluate the radiation level of the nuclear facility. Apart from the routine supervision of the coolant activity, another way of quantification of radioactivity release from the fuel elements is the investigation of spherical elements discharged from a pebble bed reactor or irradiated in a Material Test Reactor (MTR). Wenzel et al. (1979) measured the content and radial distribution of Carbon-14 (C-14) in spent fuel spheres experimentally and indicated that 96% of the C-14 was produced in the matrix graphite of the fuel spheres in Arbeitsgemeinschaft Versuchsreaktor (AVR). Schenk et al. (1988) went even further and examined in numerous experiments the transient fission products release behavior and concentration profiles of fission products in fuel spheres heated under simulated accident conditions (IAEA, 1997; IAEA, 2012).

The 10 MW high temperature gas-cooled test reactor (HTR-10) is the first gas-cooled pebble-bed reactor in China, which has been designed, built and operated by the Institute of Nuclear and New Energy Technology (INET), Tsinghua University, China (Wu and Zhang, 2004). It is a helium-cooled, graphite-moderated, and thermal neutron spectrum reactor, adopting the concept of 60 mm diameter spherical fuel elements which contain tristructural-isotropic (TRISO) coated fuel particles (Tang et al., 2002). The primary helium pressure, the core inlet temperature, the core outlet temperature, and the primary coolant flow rate of HTR-10 were 3.0 MPa, 250 °C, 700 °C, and 4.32 kg/s, respectively (Wu et al., 2002). In December 2000, HTR-10 reached first criticality, and since 2003, it was successfully demonstrating the expected safety features of a pebble bed HTGR in various experiments (Zhang et al., 2009). From July 2007 to November 2014, HTR-10 was shut down. During the year of 2015, HTR-10 was operated at 2.9 MW for about 90 days for the training of personnel that will operate the HTR-PM, the first high temperature gas-cooled reactor pebble-bed module demonstration at commercial scale in China. Before 2014, the HTR-10 was operated about 225 equivalent full power days. As a test

* Corresponding author.
E-mail address: fxie@tsinghua.edu.cn (F. Xie).

http://dx.doi.org/10.1016/j.nucengdes.2017.07.033
Received 15 March 2017; Received in revised form 12 June 2017; Accepted 28 July 2017
0029-5493/ © 2017 Elsevier B.V. All rights reserved.

reactor, the HTR-10 was used to conduct experimental measurement on the activity concentration of radioactive dust, H-3 and C-14 in the primary loop which supplied valuable data for the source term analysis in HTR-10 and HTR-PM (Wei et al., 2016; Xie et al., 2015).

In the equilibrium core of HTR-10, there are 27,000 fuel elements totally. The initial load of fuel elements into the reactor contains a fraction of 47% of graphite spheres without coated particles inside serving as moderator. During the transition to the equilibrium core, graphite spheres will be gradually discharged from the reactor and replaced with fuel elements. Since the spent fuel element from the reactor core will possess strong radiation, it is difficult to measure the nuclides in the fuel element directly. However, graphite spheres which have experienced the same neutron radiation and are composed of the same matrix graphite material, will be the ideal substitute to study the source term from the matrix material in the fuel element. The graphite matrix is made up of natural graphite, electro graphite and resin in a certain percentage (Zhao et al., 2006). In this paper, we report the complete measurement results for an irradiated graphite sphere from HTR-10 reactor core. The experimental data include the total α/β counting measurement and the absolute activity measurement with a liquid scintillation counter and a high-purity germanium detector connected to a multichannel analyzer. The distribution of the specific activity of key nuclides in the sphere are determined experimentally. Theoretical calculations for the specific activity of each nuclide are provided with the parameters from the design data and/or experimental values. By comparing the calculational and experimental results, the generation source and reduction method of fission and activation products in the matrix graphite are proposed, which can provide useful research reference for the decommissioning work and waste minimization of HTGRs.

2. Experiment

During the shutdown stage of HTR-10, several graphite spheres from the reactor core were discharged in 2014 for experimental research. To determine the distribution of the nuclides in the matrix graphite, the graphite samples at different radial positions of the sphere need to be prepared (Wang et al., 2014). A mechanical method to disintegrate the graphite sphere has been proposed. A homemade drilling machine (SIEG SUPER X3, from Shanghai SIEG Machinery Co., Ltd) with a special annular drill of which the inner diameter is 9 mm was adopted and the cylindrical graphite stick sample through the center of the irradiated graphite sphere was obtained, as indicated in Fig. 1. Then a series of graphite powder samples at unique positions of the graphite sphere were formed with a grinder machine.

The graphite powder samples were first measured with a total α/β analyzer (BH1216III, from CNNC Beijing Nuclear Instrument Factory) and a high-purity germanium detector connected to a multichannel analyzer (GC3018 detector, from Canberra Company), which are non-destructive examination methods. The total β counting rate for each graphite sample provides the qualitative radial distribution information about nuclides in the sphere. The γ spectra supply energy peaks and positions of γ emitter nuclides in the sphere. However, pure β emitting nuclides, such as H-3 and C-14, must be investigated in a further process where the graphite samples are put into a combustion vessel vented with oxygen (1180B, from Parr Instrument Company). After the combustion, H-3 and C-14 in the graphite are converted into $^{14}CO_2$ and water vapor, and adsorbed with NaOH solution in the combustion vessel completely. Then the aqueous samples were analyzed with an automatic potentiometric titrator (809Titrando, from Metrohm Company) to determine the total carbon content and a liquid scintillation counter (Quantulus 1220, from Perkin Elmer Company) to measure the activity of H-3 and C-14 in the liquid sample. The specific activity of H-3 and C-14 in the solid graphite sample can be deduced quantitatively. The conversion efficiencies during the combustion and adsorption process have been considered strictly. The detail information about the whole experimental method for the source term analysis of the graphite sphere of HTR-10 will be published in a separate paper (Liu et al., 2017).

Fig. 1. Drilling machine with a special annular drill and cylindrical graphite stick sample of the irradiated graphite sphere of HTR-10.

3. Results and discussions

3.1. Experimental results

The spectrum of the total β counting rate per gram along with the position of the sample in the graphite stick from the irradiated sphere of HTR-10 is shown in Fig. 2. It indicates that the counting rate at the surface is higher and in the interior of the irradiated sphere is nearly uniform. This phenomena can be explained by a homogenous distribution of the β-radioactive nuclides inside the irradiated graphite sphere except at the surface which is an interface between the graphite spheres and primary helium or other materials. The total α/β counting measurement can supply a qualitative distribution of the aggregate activity in the graphite sphere, whereas the information about specific nuclides needs to be investigated with a high-purity germanium detector and a liquid scintillation counter which can distinguish different types of nuclides.

Fig. 3 exhibits the β spectra of the graphite sample at 36.60 mm position of the graphite sphere from the measurement with a liquid scintillation counter. The separate peaks indicated in the spectra belong to H-3 and C-14. Fig. 4 shows the radial distribution of the specific activity of H-3 and C-14 in the irradiated graphite sphere. In the interior

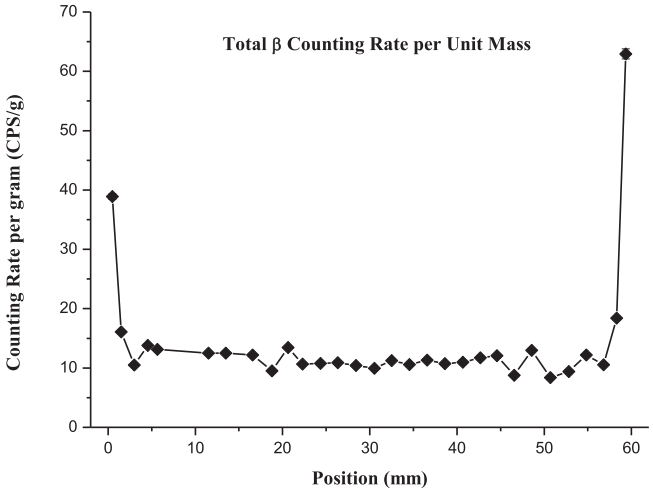

Fig. 2. Radial distribution of total β counting rate per unit mass of the irradiated graphite sphere of HTR-10.

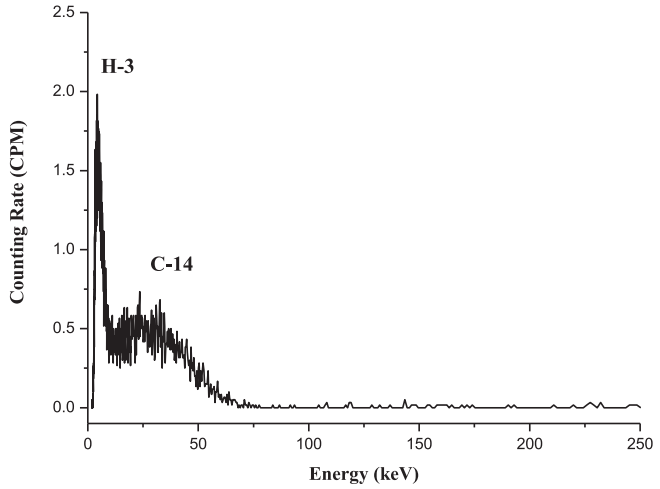

Fig. 3. β spectra of the graphite sample at 36.60 mm position of the irradiated graphite sphere of HTR-10.

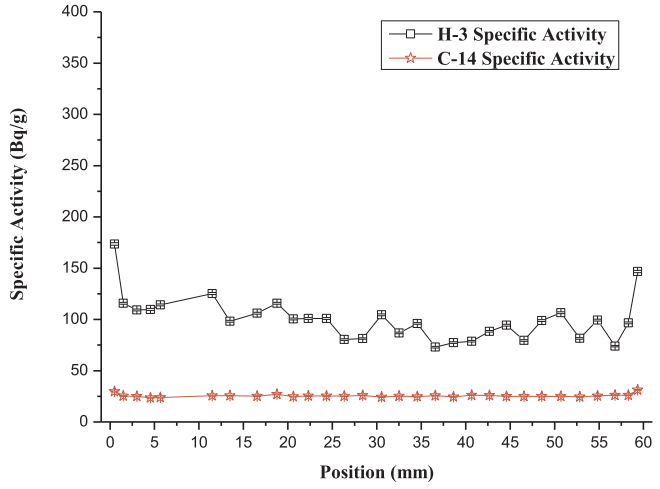

Fig. 4. Radial distribution of the specific activity of H-3 and C-14 of the irradiated graphite sphere of HTR-10.

of the graphite sphere, the specific activity of H-3 is about 96 Bq/g on the average and exhibits a nearly even distribution with small fluctuations. At the surface of the graphite sphere, the specific activity of H-3 is higher than 150 Bq/g. In contrast, the distribution of C-14 in the graphite sphere is much more uniform with a slightly higher concentration at the surface. The average specific activity of C-14 is about 25 Bq/g. The experimental data of specific activity, uncertainty, and efficiency of H-3 and C-14 along with the radial position in the irradiated graphite sphere are listed in Table 1.

Fig. 5 exhibits the γ spectra of the graphite sample at 36.60 mm position of the graphite sphere from the measurement of a high-purity germanium detector connected to a multichannel analyzer. The peak at the position of 661.7 keV indicates the nuclide Cs-137 and the peaks at 1173.2 keV and 1332.6 keV indicate the nuclide Co-60. The peaks at the position of 241.9 keV, 295.2 keV, and 351.9 keV indicate the nuclide Pb-214, the peak at 609.3 keV indicates the nuclide Bi-214, and the peak at 1460.8 keV indicates the nuclide K-40. The Pb-214, Bi-214, and K-40 are natural radionuclides. Fig. 6 shows the radial distribution of the specific activity of Co-60 and Cs-137 of the irradiated graphite sphere of HTR-10. In the interior of the graphite sphere, the specific activity of Co-60 is about 26 Bq/g on average and exhibits a nearly even distribution. But at the surface of the graphite sphere, the specific activity of Co-60 can reach values as high as 550 Bq/g. However, the distribution of Cs-137 in the graphite sphere is rather uniform. The average specific activity of Cs-137 is about 5.0 Bq/g. The experimental data of specific activity and uncertainty of Co-60 and Cs-137 along with the radial position of the irradiated graphite sphere of HTR-10 are listed in Table 2.

3.2. Comparison with theoretical calculations

3.2.1. Calculation of specific activity of H-3

The source term analysis of H-3 in HTR-10 has been analyzed by Xu et al. (2017). In the graphite materials of HTGRs, H-3 can be produced by the activation reactions of impurities in the graphite, such as Li-6, Li-7, and B-10 (Gainey, 1976; Steinwarz et al., 1980, 1984). The production rate of H-3 in the graphite sphere of HTR-10, R_T^G, can be expressed by the following equation,

$$R_T^G = \frac{dN_T^{G,Li-6}}{dt} + \frac{dN_T^{G,Li-7}}{dt} + \frac{dN_T^{G,B-10}}{dt} \quad (1)$$

where $N_T^{G,Li-6}$, $N_T^{G,Li-7}$, and $N_T^{G,B-10}$ are the numbers of H-3 atoms produced by the activation reaction of Li-6, Li-7, and B-10 in the matrix graphite, respectively.

Considering decay of H-3, the production rates of H-3 from Li-6 and Li-7 can be described as,

$$\frac{dN_T^{G,Li-6}}{dt} = \sigma_{Li-6}\phi_{Th}N_{G,Li-6} - \lambda_T N_T^{G,Li-6} \quad (2)$$

$$\frac{dN_{G,Li-6}}{dt} = -\sigma_{Li-6}\phi_{Th}N_{G,Li-6} \quad (3)$$

$$\frac{dN_T^{G,Li-7}}{dt} = \sigma_{Li-7}\phi_F N_{G,Li-7} - \lambda_T N_T^{G,Li-7} \quad (4)$$

$$\frac{dN_{G,Li-7}}{dt} = -\sigma_{Li-7}\phi_F N_{G,Li-7} \quad (5)$$

where $N_{G,Li-6}$ is the number of Li-6 atoms in the graphite sphere, σ_{Li-6} is the cross section of the activation reaction of Li-6 (n, α) H-3 (barn), ϕ_{Th} is the average thermal neutron fluence rate in the graphite sphere in the core ($cm^{-2}\cdot s^{-1}$), λ_T is the decay constant of H-3 (s^{-1}), $N_{G,Li-7}$ is the number of Li-7 atoms in the graphite sphere, σ_{Li-7} is the cross section of the activation reaction of Li-7 (n, nα) H-3 (barn), and ϕ_F is the average fast neutron fluence rate in the graphite sphere in the core ($cm^{-2}\cdot s^{-1}$).

Since H-3 can be generated from the B-10 activation by two ways, that is, directly from the activation reaction of B-10 (n, 2α) H-3 or indirectly according to the chain of activation reactions of B-10 (n, α) Li-7 and Li-7 (n, nα) H-3, the H-3 production rate equation can be described as,

$$\frac{dN_T^{G,B-10}}{dt} = \sigma_{(n,2\alpha)B-10}\phi_F N_{G,B-10} + \sigma_{Li-7}\phi_F N_{Li-7}^{G,B-10} - \lambda_T N_T^{G,B-10} \quad (6)$$

$$\frac{dN_{G,B-10}}{dt} = -(\sigma_{(n,2\alpha)B-10}\phi_F + \sigma_{(n,\alpha)B-10}\phi_{Th})\cdot N_{G,B-10} \quad (7)$$

$$\frac{dN_{Li-7}^{G,B-10}}{dt} = \sigma_{(n,\alpha)B-10}\phi_{Th}N_{G,B-10} - \sigma_{Li-7}\phi_F N_{Li-7}^{G,B-10} \quad (8)$$

where $N_{G,B-10}$ is the number of B-10 atoms in the graphite sphere, $N_{Li-7}^{G,B-10}$ is the number of Li-7 atoms produced by the B-10 activation in the graphite sphere, $\sigma_{(n,2\alpha)B-10}$ is the cross section of the activation reaction of B-10 (n, 2α) H-3 (barn), and $\sigma_{(n,\alpha)B-10}$ is the cross section of the activation reaction of B-10 (n, α) Li-7 (barn).

The specific activity of H-3 generated in the irradiated graphite sphere of HTR-10, $\overline{A}_T$, can be described as,

$$\overline{A}_T = \lambda_T\cdot(N_T^{G,Li-6} + N_T^{G,Li-7} + N_T^{G,B-10})/m \quad (9)$$

where m is the mass of the graphite sphere (g).

The average specific activity of H-3 in the irradiated graphite sphere of HTR-10 can be computed as 1.46×10^3 Bq/g by adopting the parameters listed in Table 3. Compared with the experimental value

Table 1
Experimental data of specific activity, uncertainty and efficiency of H-3 and C-14 along with the radial position of the irradiated graphite sphere of HTR-10.

Position	Weight	H-3			C-14		
		Efficiency	Specific Activity	Uncertainty	Efficiency	Specific Activity	Uncertainty
mm	g	%	Bq/g	Bq/g	%	Bq/g	Bq/g
59.34	0.0937	39.39	146.71	1.07	43.36	31.32	0.47
58.30	0.0978	39.32	96.69	0.88	43.18	26.16	0.44
56.80	0.1027	39.77	73.97	0.71	44.40	26.14	0.40
54.83	0.0977	39.88	99.31	0.87	44.68	25.47	0.42
52.84	0.0983	39.99	81.55	0.77	44.98	24.42	0.40
50.71	0.0964	39.75	106.45	0.90	44.35	24.93	0.41
48.57	0.0951	39.78	98.88	0.87	44.42	24.83	0.41
46.56	0.0965	39.76	79.53	0.79	44.36	24.85	0.42
44.59	0.0971	39.85	94.37	0.84	44.61	24.88	0.41
42.68	0.0989	39.53	88.42	0.80	43.75	25.89	0.41
40.68	0.1000	39.55	78.76	0.77	43.80	26.16	0.42
38.63	0.0999	39.74	77.41	0.74	44.32	24.47	0.40
36.60	0.0990	39.38	72.96	0.72	43.35	25.72	0.41
34.56	0.0964	40.03	96.02	0.83	45.09	24.72	0.40
32.53	0.0959	39.29	86.79	0.80	43.10	25.09	0.41
30.54	0.0967	39.52	104.43	0.88	43.73	24.23	0.40
28.42	0.1007	39.52	81.35	0.77	43.71	25.93	0.41
26.35	0.0985	39.61	80.40	0.77	43.97	25.08	0.41
24.35	0.0941	39.40	100.88	0.88	43.38	25.29	0.42
22.30	0.0947	39.61	100.84	0.86	43.95	25.35	0.41
20.63	0.0948	39.46	100.47	0.86	43.55	24.76	0.41
18.78	0.0948	39.11	115.75	0.96	42.62	26.95	0.44
16.56	0.0963	39.74	106.16	0.90	44.30	25.28	0.41
13.50	0.0959	39.86	98.23	0.88	44.64	25.51	0.43
11.50	0.0955	39.92	125.21	0.97	44.80	25.66	0.42
5.65	0.0954	39.83	114.21	0.92	44.56	23.80	0.40
4.55	0.0950	39.27	109.76	0.92	43.04	23.57	0.41
3.01	0.1010	39.67	109.11	0.90	44.12	24.88	0.41
1.50	0.0985	39.68	115.74	0.94	44.16	25.44	0.42
0.50	0.0952	39.84	173.59	1.17	44.58	29.67	0.46

96 Bq/g, the calculation result is much higher, although the average experimental measurement data of Li mass fraction in the graphite sphere has been adopted. Reason may be the uncertainties in neutron fluence rate and Li mass fraction for a specific graphite sphere which cannot be determined exactly. Also the dwell time for the graphite sphere in the core is not exactly known and conservatively assumed as the equivalent full power operation time of the reactor. Most parameters are cited from the Final Safety Analysis Report of HTR-10. However, the average experimental measurement data available of Li mass fraction in the graphite sphere is used which is much less than the design value, 0.3 ppm. The average experimental measurement data available of B mass fraction in the graphite sphere is adopted which is also much less than the design value, 3.0 ppm.

From the calculation, the H-3 generated from the Li-7 activation was two orders of magnitude less than that from the Li-6 activation, which has been analyzed by Xu et al. (2017). The specific activity of H-3 generated from the B-10 activation is about one order of magnitude less than that of Li-6. Therefore, the content of Li-6 in graphite materials has a significant effect on the specific activity of H-3 in the irradiated sphere.

3.2.2. Calculation of specific activity of C-14

In the graphite sphere of HTGRs, C-14 is produced by activation reactions of impurities in the graphite, such as C-13 and N-14 (Wang et al., 2014). Considering the generation source and decay of C-14, the production rate of C-14 in the graphite sphere of HTR-10, R^{G}_{C-14}, can be calculated by the following equations,

$$R^{G}_{C-14} = \frac{dN^{G,C-13}_{C-14}}{dt} + \frac{dN^{G,N-14}_{C-14}}{dt} \tag{10}$$

$$\frac{dN^{G,C-13}_{C-14}}{dt} = \sigma_{C-13}\phi_{Th}N_{G,C-13} - \lambda_{C-14}N^{G,C-13}_{C-14} \tag{11}$$

$$\frac{dN_{G,C-13}}{dt} = -\sigma_{C-13}\phi_{Th}N_{G,C-13} \tag{12}$$

$$\frac{dN^{G,N-14}_{C-14}}{dt} = \sigma_{N-14}\phi_{Th}N_{G,N-14} - \lambda_{C-14}N^{G,N-14}_{C-14} \tag{13}$$

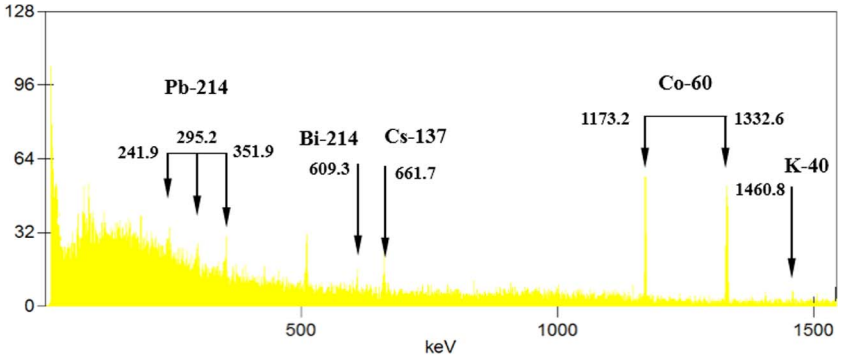

Fig. 5. γ spectra of the graphite sample at 36.60 mm position of the irradiated graphite sphere of HTR-10.

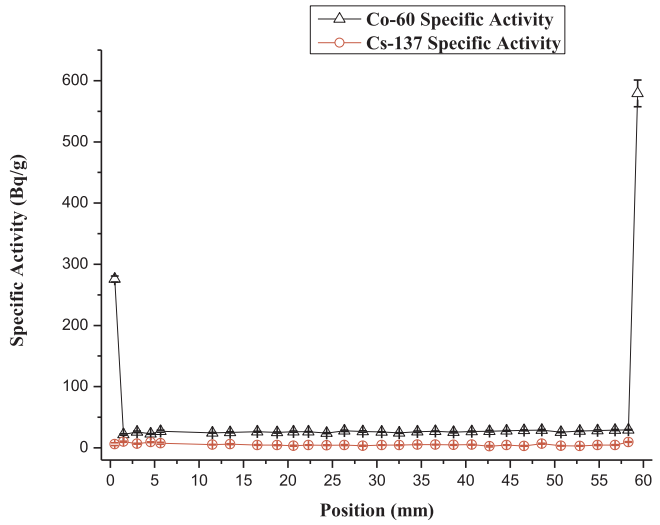

Fig. 6. Radial distribution of the specific activity of Co-60 and Cs-137 of the irradiated graphite sphere of HTR-10.

Table 2
Experimental data of specific activity and uncertainty of Co-60 and Cs-137 along with the radial position of the irradiated graphite sphere of HTR-10.

Position	Weight	Co-60		Cs-137	
		Specific Activity	Uncertainty	Specific Activity	Uncertainty
mm	g	Bq/g	Bq/g	Bq/g	Bq/g
59.34	0.0966	579.18	21.78	\	\
58.30	0.1200	29.49	0.57	9.46	0.47
56.80	0.2214	29.09	0.79	4.53	0.54
54.83	0.2523	28.25	1.06	4.44	0.71
52.84	0.2463	27.45	0.72	3.11	0.50
50.71	0.2825	25.37	0.58	3.48	0.38
48.57	0.2258	28.82	1.16	6.67	0.72
46.56	0.2554	28.47	0.73	3.14	0.49
44.59	0.2338	27.86	0.66	4.55	0.45
42.68	0.2185	27.15	1.39	2.58	1.00
40.68	0.2477	26.58	0.71	5.05	0.47
38.63	0.2541	25.43	1.08	4.66	0.73
36.60	0.2231	27.19	0.38	5.21	0.26
34.56	0.2556	26.33	1.02	5.36	0.63
32.53	0.2291	24.26	0.70	4.28	0.50
30.54	0.2512	25.96	0.44	4.55	0.29
28.42	0.2535	26.64	1.01	3.42	0.77
26.35	0.2374	27.85	1.11	4.31	0.76
24.35	0.2403	24.03	0.70	4.17	0.50
22.30	0.2411	26.15	0.37	4.42	0.25
20.63	0.1762	26.49	0.81	3.36	0.66
18.78	0.2958	25.06	0.98	4.34	0.57
16.56	0.2087	26.17	0.78	4.62	0.57
13.50	0.1768	25.31	0.83	5.98	0.59
11.50	0.1752	24.58	0.43	5.22	0.33
5.65	0.1270	27.12	1.63	7.40	1.49
4.55	0.1273	22.72	0.52	9.19	0.44
3.01	0.2076	26.00	1.29	6.79	0.82
1.50	0.1216	21.84	1.06	9.93	0.86
0.50	0.1053	275.93	4.99	6.01	2.40

$$\frac{dN_{G,N-14}}{dt} = -\sigma_{N-14}\phi_{Th}N_{G,N-14} \tag{14}$$

where $N_{C-14}^{G,C-13}$ and $N_{C-14}^{G,N-14}$ are the numbers of C-14 atoms produced by the activation reaction of C-13 and N-14 in the graphite sphere separately, σ_{C-13} is the cross section of the activation reaction of C-13 (n, γ) C-14 (barn), $N_{G,C-13}$ is the number of C-13 atoms in the graphite sphere, σ_{N-14} is the cross section of the activation reaction of N-14 (n, p) C-14 (barn), $N_{G,N-14}$ is the number of N-14 atoms in the graphite sphere, and λ_{C-14} is the decay constant of C-14 (s^{-1}).

Table 3
Main Parameters for the H-3 calculation in the irradiated graphite sphere of HTR-10.

Item	Value
Average Li mass fraction in the graphite sphere	0.0004997 ppm
Average B mass fraction in the graphite sphere	0.6749 ppm
Cross section of the activation reaction of Li-6 (n, α) H-3	942 barn
Cross section of the activation reaction of Li-7 (n, nα) H-3	0.15 barn
Cross section of the activation reaction of B-10 (n, 2α) H-3	0.05 barn
Cross section of the activation reaction of B-10 (n, α) Li-7	3838 barn
Average thermal neutron fluence rate in the core	3.45E+13 $cm^{-2}\cdot s^{-1}$
Average fast neutron fluence rate in the core	1.44E+13 $cm^{-2}\cdot s^{-1}$
Average dwell time for the graphite sphere in the core	225 d
Mass of the graphite sphere of HTR-10	199 g

Table 4
Main parameters for the C-14 calculation in the irradiated graphite sphere of HTR-10.

Item	Value
N mass fraction in the graphite sphere	13 ppm
Cross section of the activation reaction of C-13 (n, γ) C-14	9E-4 barn
Cross section of the activation reaction of N-14 (n, p) C-14	1.82 barn

The specific activity of C-14 generated in the irradiated graphite sphere of HTR-10, $\overline{A}_{C-14}$, can be deduced with the formula,

$$\overline{A}_{C-14} = \lambda_{C-14}\cdot(N_{C-14}^{G,C-13} + N_{C-14}^{G,N-14})/m \tag{15}$$

The main parameters used in the calculation are listed in Table 4. The average specific activity of C-14 in the graphite sphere has been computed as 3.64×10^3 Bq/g, which is much higher than the experimental value, 25 Bq/g. In the calculation, the C-14 produced from the C-13 activation is about 1.03×10^3 Bq/g, which depends on the exact neutron fluence rate and the dwell time in the core for the specific graphite sphere. However, the C-14 produced from the N-14 activation is affected by not only the neutron fluence rate and dwell time in the core for the graphite sphere but also the N mass fraction. We adopted the 13 ppm for the N mass fraction which was determined for the AVR graphite sphere (Wenzel et al., 1979). If the content of the N-14 in the graphite sphere can be decreased, the specific activity of C-14 could be reduced remarkably.

3.2.3. Calculation of specific activity of Co-60

In the graphite sphere of HTGRs, Co-60 is produced by the activation reactions of impurities in the graphite, such as Co-59 and Ni-60 (Wang et al., 2015). Considering the generation source and decay of Co-60, the production rate of Co-60 in the graphite sphere of HTR-10, R_{Co-60}^{G}, can be calculated by the following equations,

$$R_{Co-60}^{G} = \frac{dN_{Co-60}^{G,Co-59}}{dt} + \frac{dN_{Co-60}^{G,Ni-60}}{dt} \tag{16}$$

$$\frac{dN_{Co-60}^{G,Co-59}}{dt} = \sigma_{Co-59}\phi_{Th}N_{G,Co-59} - \lambda_{Co-60}N_{Co-60}^{G,Co-59} \tag{17}$$

$$\frac{dN_{G,Co-59}}{dt} = -\sigma_{Co-59}\phi_{Th}N_{G,Co-59} \tag{18}$$

$$\frac{dN_{Co-60}^{G,Ni-60}}{dt} = \sigma_{Ni-60}\phi_{F}N_{G,Ni-60} - \lambda_{Co-60}N_{Co-60}^{G,Ni-60} \tag{19}$$

$$\frac{dN_{G,Ni-60}}{dt} = -\sigma_{Ni-60}\phi_{F}N_{G,Ni-60} \tag{20}$$

where $N_{Co-60}^{G,Co-59}$ and $N_{Co-60}^{G,Ni-60}$ are the numbers of Co-60 atoms produced by the activation reaction of Co-59 and Ni-60 in the graphite sphere individually, $N_{G,Co-59}$ is the number of Co-59 atoms in the graphite sphere, σ_{Co-59} is the cross section of the activation reaction of Co-59 (n, γ) Co-60 (barn), $N_{G,Ni-60}$ is the number of Ni-60 atoms in the graphite sphere, σ_{Ni-60} is the cross section of the activation reaction of Ni-60 (n,

Table 5
Main parameters for the Co-60 calculation in the irradiated graphite sphere of HTR-10.

Item	Value
Average Co mass fraction in the graphite sphere	0.006483 ppm
Average Ni mass fraction in the graphite sphere	0.04662 ppm
Cross section of the activation reaction of Co-59 (n, γ) Co-60	37.18 barn
Cross section of the activation reaction of Ni-60 (n, p) Co-60	0.13 barn

p) Co-60 (barn), and λ_{Co-60} is the decay constant of Co-60 (s^{-1}).

The specific activity of Co-60 generated in the irradiated graphite sphere of HTR-10, $\overline{A}_{Co-60}$, can be deduced with the formula,

$$\overline{A}_{Co-60} = \lambda_{Co-60} \cdot (N_{Co-60}^{G,Co-59} + N_{Co-60}^{G,Ni-60})/m \quad (21)$$

The main parameters used in the calculations are listed in Table 5. The experimental values for the Co and Ni mass fractions in the graphite sphere are adopted. The average specific activity of Co-60 in an irradiated graphite sphere of HTR-10 can be computed as 1.14×10^3 Bq/g, which is much higher than the experimental value, 26 Bq/g. From the calculation, the Co-60 from the Ni-60 activation only contributes 3.18 Bq/g. It indicates that the content of Co-59 in the graphite matrix makes significant effect on the specific activity of Co-60 in the irradiated graphite sphere.

3.2.4. Calculation of specific activity of Cs-137

Although there are no TRISO coated particles inside the graphite sphere, natural uranium contamination exists in the matrix graphite. The fraction of natural U-235 in the matrix graphite to the U-235 in a fuel element of HTR-10 is estimated as 7.0×10^{-7}. From the Final Safety Analysis Report of HTR-10, the activity of Cs-137 in the spent fuel element is 4.98×10^{10} Bq. For each spent fuel element, it has experienced 1175 days in the core at full power operation of HTR-10. Assuming Cs-137 in the matrix graphite of the graphite sphere mainly comes from the fission reaction of the natural uranium, the specific activity of Cs-137 in an irradiated graphite sphere of HTR-10 with 225 equivalent full power days can be estimated as 25 Bq/g, which is a little higher than the experimental value, 5 Bq/g.

3.3. Discussion

From current experiments, the source terms in the irradiated graphite sphere of HTR-10 include H-3, C-14, Co-60, and Cs-137. The experimental specific activities in the interior of the sphere are about 96 Bq/g, 25 Bq/g, 26 Bq/g and 5 Bq/g for H-3, C-14, Co-60 and Cs-137, respectively. The current results indicate that the activity concentrations in the matrix graphite of HTR-10 are much less than those of AVR nuclear graphite of the reflector, which are about 884,000 Bq/g, 95,000 Bq/g, 27,000 Bq/g, and 1940 Bq/g for H-3, C-14, Co-60 and Cs-137 (Fachinger et al., 2008). The possible reasons may be various types of fuel elements of lower compared to today's quality including bistructural-isotropic (BISO) coated particles were adopted in AVR. The AVR reactor was operated at a very high temperatures, ~950 °C, for certain time, which can lead to the promotion of the diffusion of fission or activation products in the core. The impurities in the graphite materials may be not seriously controlled at that time. Thus, the average activity concentration of nuclides in the primary loop and also in the graphite materials were substantially increased (Bäumer and Barnert, 1990).

The distribution of nuclides in the interior of the irradiated graphite sphere of HTR-10 is nearly homogenous which can be understood, as the impurities and the natural uranium in the matrix graphite are evenly distributed. However, the concentrations of H-3 and Co-60 at the surface of the irradiated graphite sphere are a little higher than the internal, showing that a part of these nuclides has also an origin outside the sphere.

Unlike the experimental result of C-14 in AVR fuel spheres whose surface has a much higher concentration, the C-14 in the irradiated graphite sphere of HTR-10 is nearly homogeneously distributed with a slightly higher concentration at the surface. The reason may lie in the fact that the content of nitrogen impurities in the cooling gas of HTR-10 is much lower than that of AVR. The experimental measurement of the activity concentration of C-14 in the primary loop of HTR-10 is about three orders of magnitude less than that of AVR and the related research results will be published elsewhere. The average specific activity of C-14 in the matrix graphite of fuel elements of AVR is about 3.7×10^4 Bq/g compared with the 26 Bq/g experimental value in the graphite sphere of HTR-10 (Wenzel et al., 1979).

The Cs-137 can be produced by the fission reaction of natural uranium contamination in the matrix graphite. Another possibility could be that the Cs-137 from the fuel elements co-resident in the reactor first was released into the primary coolant, and then adsorbed and diffused in the graphite spheres. With the experimental measurement data of HTR-10 and the Cs-137 diffusion experiments in the graphite available (Hayashi et al., 1987; Carter et al., 2015, 2016), we thought the release, absorption and diffusion processes of Cs-137 in the graphite material around 600 °C (the average temperature of fuel elements in the core of HTR-10) could be slow. Most of the Cs-137 observed in the current experiment probably comes from the fission reaction of natural uranium contamination in the matrix graphite. The nearly homogenous distribution of Cs-137 in the irradiated graphite sphere of HTR-10 can be understood that natural uranium are well distributed in the matrix graphite. The release, absorption and diffusion behaviors of Cs-137 in the real irradiated graphite sphere are worth investigating and under consideration.

Since the graphite has a strong absorption ability for H-3 and the H-3 was found to be more soluble in graphite than in helium, the surface of the graphite sphere may serve as an interface where the interaction between H-3 in the primary loop and matrix graphite occurs (Tsetskhladze et al., 1988; Röhrig et al., 1976; Moormann, 2008). In the graphite sphere from reactor core of AVR, a similar specific activity distribution of H-3 with higher concentration near the surface was recorded which indicated the strong interaction between H-3 and graphite (Steinwarz et al., 1980).

As discussed by Humrickhouse (2011), friction and abrasion between the fuel elements and graphite spheres will happen during the movement of the pebbles in the reactor core. The friction and stick of substances of higher radioactivity from other graphite spheres and/or fuel elements could be a reason to explain the higher concentration of Co-60 at the surface of the sphere. Another possibility is that the surface contamination with high impurities such as Co-59 occurred during machining and handling of the sphere prior to irradiation, which can also result in a higher concentration of the activation product Co-60 at the surface of the sphere.

The reason for the differences between calculation results and experimental values of specific activity of nuclides in the irradiated graphite of HTR-10 lies in the difficulty to determine correctly the exact neutron fluence rate, accurate content of impurities, and explicit dwell time in the core for a specific graphite sphere. Although some average experimental values are adopted, impurities in various batches of graphite spheres of HTR-10 are different. Even in the same batch, the measurement values will exhibit a statistical distribution upon the trace analysis.

Though theoretical calculations are conservative, it can provide useful information for the generation mechanism of key nuclides in the irradiated graphite sphere in HTR-10. In the graphite sphere, the overwhelming majority of H-3 is produced by the activation of Li-6. Therefore, the control of the content of Li-6 in the matrix graphite may have a significant effect on the concentration of H-3 in the irradiated graphite sphere of HTR-10. For C-14, the contribution from C-13 is somewhat stable for it depends on the natural abundance of C-13 in the matrix graphite. However, the content of N-14 in the matrix graphite

can affect the total amount of C-14 in the irradiated graphite sphere of HTR-10 greatly. From the theoretical calculation, the dominant contribution of Co-60 is the Co-59 activation. To limit the content of Co-59 in the graphite materials can control the concentration of Co-60 in the irradiated graphite sphere of HTR-10 effectively. The total activity of the fission product Cs-137 in the irradiated graphite sphere of HTR-10 mainly depends on the natural uranium fraction in the matrix graphite. Therefore to control the natural uranium contamination in the matrix graphite can decrease the Cs-137 content in the irradiated graphite sphere of HTR-10 significantly.

More experiments on the source term of graphite spheres in HTR-10 are under consideration. With experimental data from more irradiated graphite spheres of HTR-10, the types and the distributions of nuclides in the matrix graphite can be determined more explicitly and accurately, which can shed light on the source term analysis of fuel elements and graphite materials in the reactor core of HTR-10.

4. Conclusion

With the total α/β counting measurement and the absolute activity measurement with a liquid scintillation counter and a high-purity germanium detector connected to a multichannel analyzer, the content and the radial distribution of key nuclides in an irradiated graphite sphere from the reactor core of HTR-10 have been investigated experimentally, and compared with theoretical calculations. The current studies indicate that: (1) The key nuclides in the irradiated graphite sphere of HTR-10 contain H-3, C-14, Co-60, and Cs-137; (2) The specific activities of H-3, C-14, Co-60, and Cs-137 exhibit a symmetric distribution relative to the center of the sample from the graphite sphere, and the average specific activities in the interior of current graphite sphere are about 96 Bq/g, 25 Bq/g, 26 Bq/g and 5 Bq/g for H-3, C-14, Co-60 and Cs-137, respectively; (3) The specific activities of C-14 and Cs-137 are nearly uniform in the sample from the graphite sphere; (4) The specific activities of H-3 and Co-60 are much higher at the surface than the interior of the graphite sphere.

According to the operational history of HTR-10 and the measurement or design data about the content of impurities in the graphite, the specific activities of H-3, C-14, Co-60, and Cs-137 are conservatively estimated. Combined with the experimental measurements, dominant sources of H-3 and Co-60 in the graphite sphere of HTR-10 come from the activation of Li-6 and the activation of Co-59, separately. The higher specific activity of H-3 near the surface of the graphite sphere may lie in the strong absorption interaction between graphite and tritium in the primary coolant. The higher Co-60 activity at the surface of the sphere could be explained by friction and stick of substances of higher radioactivity from other graphite spheres and/or fuel elements. And another explanation would be that the surface contamination with high impurities such as Co-59 occurred during machining and handling of the sphere prior to irradiation. The C-14 in the graphite sphere is generated from the activation of C-13 and N-14, and the content of N-14 in the graphite will have a significant effect on the amount of C-14. The Cs-137 in the graphite sphere may come from the fission reaction of natural uranium contamination, which presents a very low specific activity.

The current research can provide crucial experimental data for the source term analysis of graphite spheres and fuel elements in the reactor core of HTR-10, and supply important reference for waste minimization, radiation protection, and decommissioning work of HTGRs.

Acknowledgements

This work was supported by the National Natural Science Foundation of China (No. 11575099), the Beijing Natural Science Foundation (No. 2163051), the Tsinghua University Initiative Scientific Research Program (No. 20151080375), and the Chinese National Significant Science and Technology Project (No. ZX06901). We are grateful for the technical support from Mr. Shouang Wang, Mr. Xin Huang, Mr. Xiaogui Feng, Mr. Liqiang Wei, and fruitful discussions with Prof. Fu Li, Dr. Xiaotong Chen, Dr. Bing Xia, in INET, Tsinghua University, Beijing, China and Dr. Karl Verfondern, in Research Center Juelich, Juelich, Germany. We also thank Prof. Sudarshan K. Loyalka in Nuclear Science and Engineering Institute, University of Missouri, USA for discussion on the diffusion behavior of cesium in the graphite and sending related articles.

References

Bäumer, R., Barnert, H., 1990. AVR-Experimental High-Temperature Reactor: 21 years of Successful Operation for a Future Energy Technology. The Association of German Engineers (VDI-Verlag GmbH), Düsseldorf, Germany.

Carter, L.M., Brockman, J.D., Loyalka, S.K., Robertson, J.D., 2015. Measurement of cesium diffusion coefficients in graphite IG-110. J. Nucl. Mater. 460, 30–36.

Carter, L.M., Brockman, J.D., Robertson, J.D., Loyalka, S.K., 2016. Diffusion of cesium and iodine in compressed IG-110 graphite compacts. J. Nucl. Mater. 476, 30–35.

Fachinger, J., Lensa, W.V., Podruhzina, T., 2008. Decontamination of nuclear graphite. Nucl. Eng. Des. 238, 3086–3091.

Gainey, B.W., 1976. Review of Tritium Behavior in HTGR Systems. GA-A-13461. General Atomic Company, San Diego, California, USA.

Hayashi, K., Kobayshi, F., Minato, K., Ikava, K., Fukuda, K., 1987. In-pile release behavior of metallic fission products in graphite materials of an HTGR fuel assembly. J. Nucl. Mater. 149, 57–68.

Humrickhouse, W., 2011. HTGR dust safety issues and needs for research and development. In: INL/EXT-11-21097. Idaho National Laboratory.

IAEA, 1997. Fuel performance and fission product behavior in gas cooled reactors. IAEA-TECDOC-978, VIENNA.

IAEA, 2012. Advances in high temperature gas cooled reactor fuel technology, IAEA-TECDOC-1674, VIENNA.

Liu, X., Huang, X., Xie, F., Jia, F., Feng, X., Li, H., 2017. Source term analysis of irradiated graphite in the core of HTR-10. Sci. Technol. Nucl. Inst. 2017, 1–6 2614890.

Moormann, R., 2008. Fission product transport and source terms in HTRs: experience from AVR pebble bed reactor. Sci. Technol. Nucl. Inst. 2008, 1–14 597491.

Röhrig, H.D., Fischer, P.G., Hecker, R., 1976. Tritium balance in high-temperature gas-cooled reactor. J. Am. Ceram. Soc. 59 (7–8), 316–320.

Schenk, W., Pitzer, D., Nabielek, H., 1988. Fission product release profiles from spherical HTR fuel elements at accident temperatures. Institut für Reaktorwerkstoffe, Germany Jül-2234.

Steinwarz, W., Stöver, D., Hecker, R., Thiele, W., 1984. Distribution of tritium in a nuclear process heat plant with HTR. Nucl. Eng. Des. 78, 267–272.

Steinwarz, W.D., Rohrig, D., Nieder, R., 1980. Tritium behaviour in an HTR system based on AVR-experience. In: Specialists Meeting on Coolant Chemistry, Plate-Out and Decontamination in Gas-Cooled Reactors IWGGCR-2, Juelich, Federal Republic of Germany.

Tang, C., Tang, Y., Zhu, J., Zou, Y., Li, J., Ni, X., 2002. Design and manufacture of the fuel element for the 10 MW high temperature gas-cooled reactor. Nucl. Eng. Des. 218, 91–102.

Tsetskhladze, T.V., Cherkzishvili, L.I., Chikhladze, L.A., 1988. Interaction of tritium with graphite. Soviet Atomic Energy 64 (3), 254–258.

U.S. DOE Nuclear Energy Research Advisory Committee (NERAC) and the Generation IV International Forum (GIF), 2002. A technology roadmap for generation IV nuclear energy systems. GIF-002-00.

Wang, S., Pi, Y., Xie, F., Li, H., Cao, J., 2014. Study on ^{14}C content in post-irradiation graphite spheres of HTR-10. Atomic Energy Sci. Technol. 48 Suppl, 506–510.

Wang, S., Xie, F., Li, H., Cao, J., Li, F., Wei, L., 2015. Study on the production mechanism of Co-60 in the primary loop of HTR-10. In: Proceedings of ICONE-23 (23rd International Conference on Nuclear Engineering), Chiba, Japan.

Wei, L., Xie, F., Chen, X., Ma, T., Tong, J., Li, F., 2016. Summary and experience feedback on the restart and power operation after a long-time shutdown of HTR-10. In: Proceeding of the 8th International Topical Meeting on High Temperature Reactor Technology (HTR 2016), Las Vegas, NV, USA.

Wenzel, U., Herz, D., Schmidt, P., 1979. Determination of ^{14}C in spent HTGR fuel elements. J. Radioanal. Chem. 53 (1–2), 7–15.

Wu, Z., Lin, D., Zhong, D., 2002. The design features of the HTR-10. Nucl. Eng. Des. 218, 25–32.

Wu, Z., Zhang, Z., 2004. The Advanced Nuclear Energy System and High Temperature Gas-Cooled Reactor. Tsinghua University Press, Beijing.

Xie, F., Cao, J., Chen, Z., Dong, Y., 2015. The design and study of the radioactive graphite dust experimental system in the primary loop of the HTR-10. Atomic Energy Sci. Technol. 49, 744–749.

Xu, Y., Li, H., Xie, F., Cao, J., Tong, J., 2017. Source term analysis of tritium in HTR-10. Fusion Sci. Technol. 71, 671–678.

Zhang, Z., Wu, Z., Wang, D., Xu, Y., Sun, Y., Li, F., Dong, Y., 2009. Current status and technical description of Chinese 2 × 250 MWth HTR-PM demonstration plant. Nucl. Eng. Des. 239, 1212–1219.

Zhang, Z., Yu, S., 2002. Future HTGR developments in China after the criticality of the HTR-10. Nucl. Eng. Des. 218, 249–257.

Zhao, H., Liang, T., Zhang, J., He, J., Zou, Y., Tang, C., 2006. Manufacture and characteristics of spherical fuel elements for the HTR-10. Nucle. Eng. Des. 236, 643–647.